BEAM STEERING MECHANISM FOR EARTHCARE ATMOSPHERIC LIDAR INSTRUMENT – AN IMPROVED PIEZOELECTRIC TIP-TILT MECHANISM

Frederic Bourgain(1), Olivier Sosnicki(1), François Barillot(1), Frank Claeyssen(1)
Jean Pierre Lelay(2), Eddie Prevost(2), Thierry Pain(2), Benoit Germain(2),
(1) Cedrat Technologies S.A., 59 chemin du Vieux Chêne 38246 MEYLAN, FRANCE, Email:actuator@cedrat-tec.com
(2) Sodern, 20 Avenue Descartes B.P. 23 94451 LIMEIL-BREVANNES Cedex , Email : benoit.germain@sodern.fr

ABSTRACT

In the context of the ATLID instrument [1] embedded in the EarthCARE mission (Earth Cloud, Aerosol and Radiation Explorer), a Beam Steering Assembly is deviating a pulsed high energy UV laser beam to compensate the pointing misalignment between the emission and reception paths of ATLID with a very high stability and high resolution.
Within the EarthCARE mission, led by ESA, Astrium is responsible for the ATLID instrument. The BSA development, manufacture and tests were assigned by Astrium to Sodern, an EADS filial.

In this context, Cedrat Technologies was sub-contracted by Sodern to design, manufacture and test the performances of Beam Steering Mechanism flights models.
This paper points out the main mechanism design issues:

- High performances;
- Mechanical and thermal stability;
- Low power consumption;
- High integration level;
- High reliability and safety;
- Cleanliness requirements.

and examines how these issues have been approached by Cedrat Technologies and Sodern. Test results are reported when available.

1. INTRODUCTION

1.1. Context

ATLID (ATmospheric LIDar) is one of the four instruments of EarthCARE, it shall determine vertical profiles of cloud and aerosol physical parameters such as altitude, optical depth, backscatter ratio and depolarisation ratio.

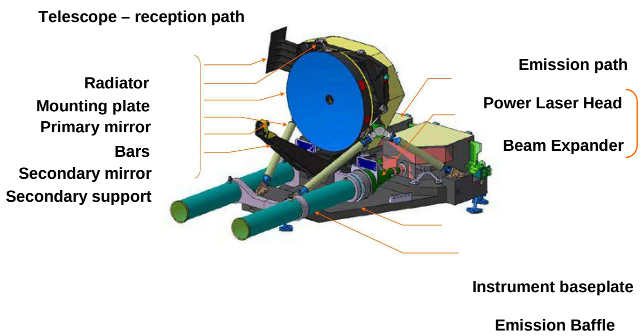

Figure 1: ATLID Instrument overview [1]

The BSA function is to compensate for the pointing misalignment between the emission and reception paths of ATLID with a very high stability, with high resolution.
The BSA is a 2-axis small range pointing mechanism, implemented in Power Laser Head Optical Bench, inside the pressurized PLH. See Fig. 2

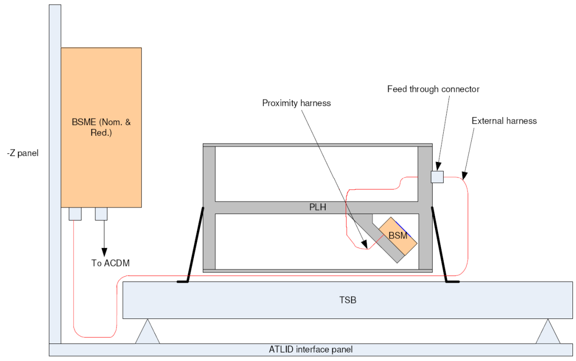

Figure 2 : BSA implantation schema

1.2. BSA description and Industrial organisation

The BSA is composed of:

- A unit including optics, mechanics and electronics (BSMFE) made of two sub-assemblies: a Mechanism equipped with the tip-tilt mirror (BSM) and Front End Electronics (BSFE), Implemented in the PLH
- An Electronics Unit (BSME), implanted on instrument panel
- A Harness (BSH) composed of two cables, connecting the two units.

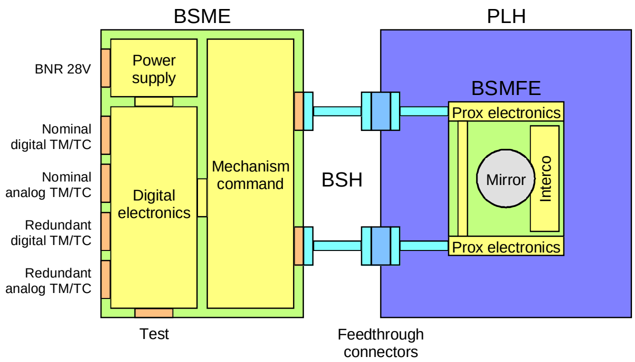

Figure 3: BSA Architecture

'15th European Space Mechanisms & Tribology Symposium – ESMATS 2013'
Noordwijk, The Netherlands, 25–27 September 2013

Sodern develops the overall BSA including the Main Electronics Unit BSME and the Front End Electronic to monitor and control the BSM in regards of the high level of stability. Sodern also performs the overall BSA tests.

Cedrat Technologies was sub-contracted by Sodern, an EADS filial, to design, manufacture and test the performances of BSM – Beam Steering Mechanism. See Fig. 4 for the exact definition of BSM perimeter.

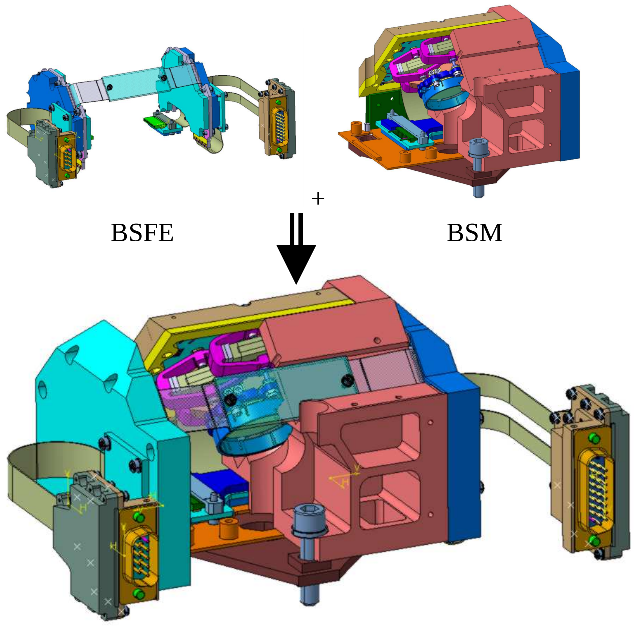

Figure 4: BSMFE overview

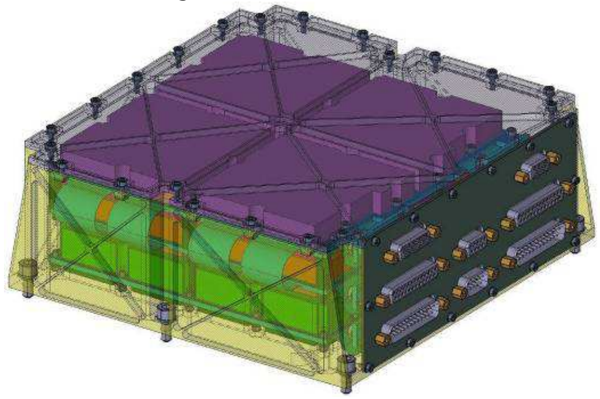

Figure 5: BSME overview

1.3. PHARAO Heritage

Both Cedrat Technologies and Sodern were already associated on PHARAO project to develop a similar mechanism [2].
PHARAO is a cold atoms space clock that includes a Laser Source whose Sodern is responsible for, under CNES contract. The Laser Source uses 8 mechanisms MEF (Flux Equilibrium Mechanism) similar to the BSM.

Their function is to align the laser beam in collimated optical fibers to adjust optical power between different channels.

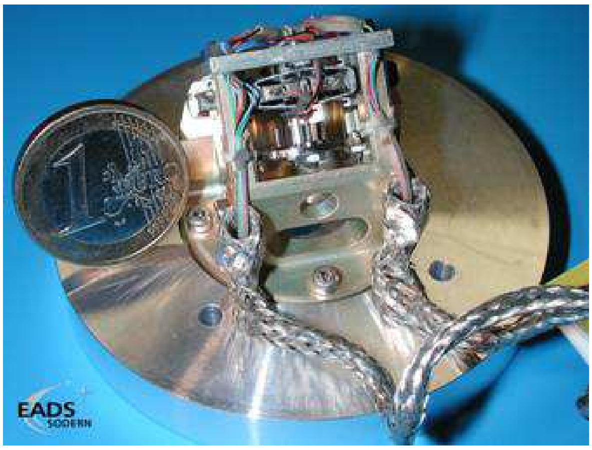

Figure 6: MEF picture

For the BSM, the main basic building blocks were reused such as mechanism push pull architecture and electronic architecture.
The most important design differences are:

- Mirror dimension: 27mm diameter for BSM instead of 4mm diameter for the MEF.
- Allowable volume, and global layout of the mechanism and electronic.

The most important improvements compared with PHARAO are listed in the table below:

Performance improvement		
	MEF PHARAO	BSM ATLID
Pointing stability	2µRad on 20 days	0.5µRad on [1mHz; 10Hz] bandwith Long term accuracy specified: 50µRad
Temperature environment	Regulated baseplate: ~10mK order of magnitude	Operationnal temperature in [24°C; 40°C] range with following stability : 4K drift on long term 1K on MT2; MT3 see Tab. 2
Long term stability	Not requested	50µRad
Repeatability	Not requested	50µRad

Table 1: Performance improvement for BSA

2. TECHNICAL CHALLENGES

As explained above, the direction of the laser beam needs to be co-aligned with the reception path of the instrument to maximize the detection of the LIDAR echo signal. The BSA should compensate for the pointing misalignment between the emission and reception paths of ATLID with a high resolution and a very high stability.

2.1. Driving requirements for the BSA

The BSM is required to steer the incoming laser beam through a range of ± 3 mrad – optical range for the two axes with a control bandwidth up to 10Hz. This performance demands a mechanical rotation of +/-2.12mrad on the Rx defined axis and +/-1.5mrad on the Ry defined axis at the BSM level.

2.2. Critical performances requirements

The critical requirements are the accuracy of the movement, the stability (short term, mid term and long term) and the repeatability.
The following table lists the time scale and associated instability contributors (Tab. 2).

Contributors to stability budgets	
Time scale	**Contributors**
Long term (LT) Lifetime: in orbit life time 37 months + on ground life time 7 Years	On ground alignment Launch micro setting Gravity release Moisture release LT thermal variations Ageing
Medium term (MT) MT1: One Month MT2: One orbit (~90min) MT3: Co-alignement closed loop (~1000.sec)	Calibrations errors Orbital thermal variations
Short term (ST) 1.5sec	ST thermal variations Measurement noise Laser angular jitter
Dynamics Laser roundtrip period (~3msec)	Spacecraft stability Spacecraft jitter

Table 2: Potential contributors to the stability.

All performance requirements shall be fulfilled for any contributors and for any optical angles (Tab. 3).

General performance requirements		
Description	**Req.**	**Unit**
Optical angular range Rx, Ry Mechanical angular range Rx Mechanical angular range Ry	+/-3 +/-2.12 +/-1.5	mrad
Thermal sensitivity: BSM contribution BSFE contribution	 7.5 1	µrad/°C
Total repeatability	100	µrad
Rx, Ry Linearity @full stroke dA_realized/dA_commanded	1 +/-5%	µrad/µrad
Power consumption: BSM contribution BSFE contribution BSME contribution	 0.2 1.3 4.5	W

Table 3: Extract of the performance requirements for the BSA (Opical Angle).

2.3. Environmental requirements

Several additional requirements make the design and the validation of the BSA quite challenging.

- Stability requirement is to be achieved while temperature may vary from +/-0.5°C on the short term to +/-2°C on the long term.
- The mechanism is to survive launch conditions (50g RMS random, 1000g shocks)
- Micro-vibration susceptibility requires to be minimised to achieve stability requirements during flight.
- The BSM shall withstand direct solar illumination without damage and shall be able to survive without permanent damage, to a solar input beam of 12W during 2 minutes.
- The BSA is located near the pulsed laser resulting in a harsh magnetic environment.
- Due to position of the BSA inside the PLH, the contamination requirements on the optical bench are strict and any outgassing materials should be avoided.

These challenging requirements necessitated to improve the mechanism design.

3. BSA DETAILED DESCRIPTIONS

The BSA design tasks were performed to develop the different parts: BSM, BSMFE and BSME.
The design optimizes the dimensions of the BSMFE in order to facilitate its implantation in PLH. Proximity electronics need to be near the actuators and sensors in order to have the same regulated temperature. See Fig. 4

3.1. Beam Steering Mechanism mechanical design

The BSM is a 2-axis Tip-Tilt mechanism (TTM), mounted on a bracket. It supports the BSFE.
The BSM is based on two stiff push pull pairs of APA60SM® actuators [3] equipped with Strain Gages (SG). It is able to produce more than +/-2.12mrad for Rx rotation and +/-1.5mrad for Ry rotation – Mechanical Angle - with a bandwidth up to 10Hz. This design allows a mechanical resonant frequency above 2kHz thus avoiding the use of a launch locking mechanism and limiting the micro-vibration susceptibility.

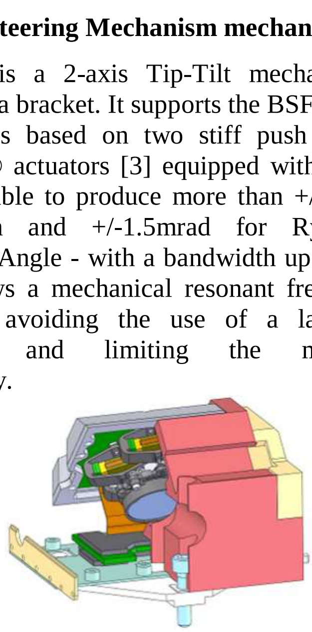

Figure 7: BSM overview

The BSM is composed of the following components:

- The bracket that is the frame of the whole BSM assembly and supporting the proximity electronics.
- The Tip-Tilt Mechanism assembly providing beam steering movements,
- The mirror with holder for mirror replacement.
- The solar shield for solar illumination protection,
- The interconnection board which is the printed circuit board connecting the different electrical signals from each APA®, securing the connections and interfacing the BSM with Front End boards,
- The covers that provide mechanical and electromagnetic protections,
- The adjustable shim for compensating machining or integration biases for the BSM and the mirror.

The position of the piezo actuators was selected to allow a different stroke between the two rotation axes. This choice enables to maximise the applied voltages on the piezo ceramics and then improve the overall sensitivity of the mechanism.
Once the piezoactuators sized, several simulations were performed to validate simultaneously angular range, stress resulting from integration, thermal environment, vibration/shocks environments and micro sliding at screwed links in regards of the thermal and vibration/shocks environments (Fig. 8). All the stress contributions were summed and complied with the ECSS safety margins for both non-operational and operational modes.

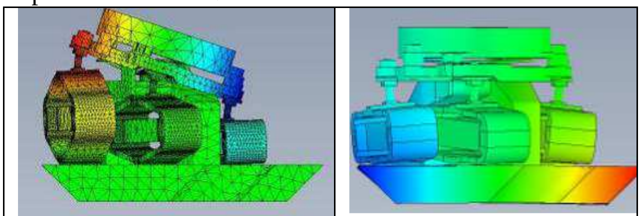

a- Calculated maximum displacements during YUmm axis actuation	*b- Thermal deformation of the TTM under 10°C variation*

Figure 8: Some results of FEM simulations

Compared to Pharao MEF, the electrical assembly has been improved to take into account the large number of electrical connections. An interconnection board was designed, using the Cedrat Technologies' heritage, to distribute the power and sensors signals. This design puts focus on balancing the Wheatstone bridge and reducing electromagnetic coupling (see 3.2 paragraph).
Concerning the cleanliness, the following design rules have been applied on each BSM parts:

- Surfaces accessible for visual inspection / cleaning,
- No blind cavities/holes,
- Use of low outgassing materials including glues (for strain gages bonding on the MLAs and for securing wires).
- Low surface roughness,
- The electrical connections using an IB board as support to simplify the cleaning of the electrical connection.

3.2. Position transducers on the BSM

The high required level of accuracy and stability for the BSA necessitated including high reliability position sensors for each axis.

Because of small allocated volume for the BSA and small deflection movement, this prohibited the use of contactless sensors like capacitive sensors. So, Cedrat Technologies has proposed a contact sensing transducer using improved strain gage elements mounted in the well known Wheatstone Bridge and glued directly on the piezoelectric ceramics (Fig. 10). The single element was selected in regards of the maximum stress supported in the ceramic (up to 1000ppm) and the required ageing.

Concerning the sensing material of the strain gage, the constantan alloy is chosen to improve the variation of the resistance of the strain gage with the strain and to have a linear response of the output voltage versus strain. Additionally, constantan based strain gages are characterised by good life time and its temperature coefficient of resistance is not excessive.

To improve the accuracy and the stability of the strain gage measurements, several precautions were brought. A full bridge configuration was selected to improve the sensitivity while limiting the thermal impact and non linearity errors on its performance (Fig. 9). The initial sensitivity is given in Eq.1.

$$\frac{\Delta R}{R} = GF_x \times (\varepsilon_{strain}) \quad (1)$$

$$Vout = Excitation \times \left(\frac{R4}{R3+R4} - \frac{R2}{R2+R1}\right) \quad (2)$$

With $R_{1,3} = R_0 - \Delta R$, $R_{2,4} = R_0 + \Delta R$

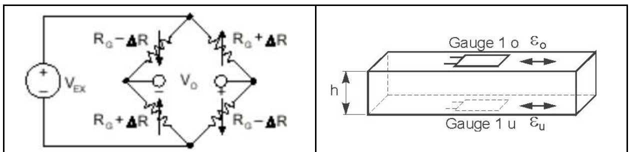

a- Standard full bridge configuration	*b- Proposed mounting configuration on one ceramic*

Figure 9: Selected Full bridge configuration and its application on the push pull piezomechanism

The full bridge configuration is theoretically insensitive to temperature effect du to the well symmetric bridge.
From the previous formulae, we have introduced a thermal coefficient with an apparent strain (Eq.3).

$$\frac{\Delta R}{R} = GF_x \times (\varepsilon_{strain} + \varepsilon_{thermal}) \qquad (3)$$

If four strain gages are applied to the specimen and connected into a full bridge, the thermal component in the total strain has the same sign for all strain gages; they are all subjected to the same change in temperature. Based on Eq.2 and Eq.3, we establish the expressions (Eq.4):

$$Vout = Excitation \times \frac{SG}{4} \times [(\varepsilon_{strain} + \varepsilon_{thermal})_{\_1} - (\varepsilon_{strain} + \varepsilon_{thermal})_{\_2} + (\varepsilon_{strain} + \varepsilon_{thermal})_{\_3} - (\varepsilon_{strain} + \varepsilon_{thermal})_{\_4}]$$

$$Vout = Excitation \times \frac{SG}{4} \times 4\varepsilon_{strain} \qquad (4)$$

This theory is valid as long as no thermal gradient appears between the bridge components. The degree of the compensation depends on the uniformity of the temperature at the strain gage level. Balancing the thermal conductive paths at the bracket level is mandatory.
In order to minimise the bridges sensitivity to external drifts (thermal effect, thermocouple effect, …) the bridge should be balanced as much as possible (i.e. to null the residual offset). An adequate pairing of the ceramics + strain gage couple has been performed and allowed to reduce the initial offset by 99%.

As the principle of the position measurement is linked to the capability to see small stress through the glued interface, a specific Cedrat Technologies gluing process was used to achieve optimised repeatability by limiting dust, voids, and bubbles inside the glue interface (Fig. 4). A specific evaluation campaign was conducted to validate the gluing process (See paragraph 4).

Additional actions were taken to further improve bridge stability:

- Reduction of the power dissipation,
- Improve the alignment of the strain gages on the ceramic ,
- Balance the lead wires.

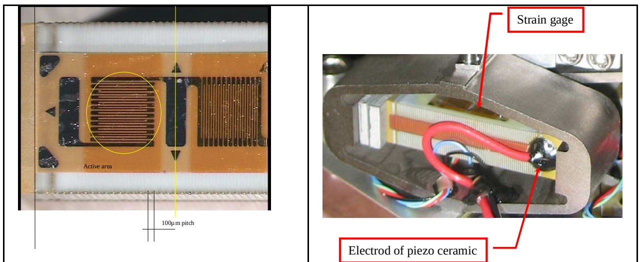

a- Strain gage glued on the piezo ceramic	b- Implementation of the SG in the APA® shell

Figure 10: Integration of the strain gage onto the APA®

Electromagnetic coupling paths have been minimized:

- Conductive (common impedance): mitigation through fine routing of the traces,
- Radiative paths: Use of specific covers including chicanes,
- Inductive coupling: Twisted wires and minimized PCB's loops areas.

3.3. Beam Steering Electronic

The BSA electronics is split in three flex-rigid PCBs:

- The Interconnection Board (IB) located inside the BSMFE behind and beneath the TTM mechanism,
- The Front End Board (FEB) located inside the BSMFE all around the BSM mechanics
- The Main Electronic Board (MEB) located inside the BSME at a 3m distance of the PLH.

3.3.1. BSFE electronics

The Front End Board (FEB) provides the most critical functions of the BSA:

- The strain gages bridges voltage conditioning
- The strain gages bridges offset compensation
- The strain gages signal amplification, which is full differential in input and output with a gain close to 2500

All these functions benefit of the best thermal conditions available on the equipment, which are however far worse than the PHARAO ones, even if the final performances expected are better, thank to TTM and electronics improvements. The PCB outlines and its routing are also particularly complex in order to be compatible with specified mechanical and electrical interface.

Others particularities or difficulties associated to the FEB electronics are the need of interchangeability and the need of cleanliness, combined with the necessity to be immune to the close high current laser pulses of more than 100A which exist beside the BSMFE.

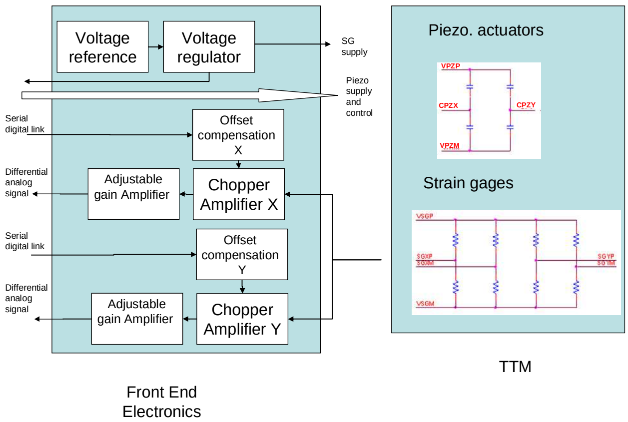

Figure 11: Front End Electronic Architecture

3.3.2. BSME electronics

The Main Electronic Board (MEB) provides the other specified functions of the BSA which can be deported far away from the mechanism:

The first part is the power supplying of all the BSA circuits by a single fully shielded dc-dc converter
The second one regroups the digital functions associated to the management by a FPGA in order to:

- Interface the ACDM units
- Configure the BSA operating modes
- Acquire the data of a single multi-channel ADC
- Drive two pairs of DACs for position setting and offset compensation,
- Manage the strain gage offset compensation process (king of self-calibration mode)
- Increase the command and control resolution by four by addition of a simple data processing

The third one regroups the analog functions associated to the mechanism command and control:

- High and low voltage secondary regulations
- High voltage power sparing amplifiers for the command of the piezoelectric actuators
- Damped sinusoid generation for the hysteresis compensation of these actuators during the strain gage offset compensation process
- Acquisition and reuse inside the MEB of the FEB voltage reference for the mechanism stability optimization
- Acquisition and processing of the FEB amplified strain gage signals for measurement or comparison with their setting point depending on the operating mode (close or open loop)
- Formatting of the digitalized signals

The outlines of this PCB are far much classical and spacious than the two others. It is simply fold inside the BSME case.

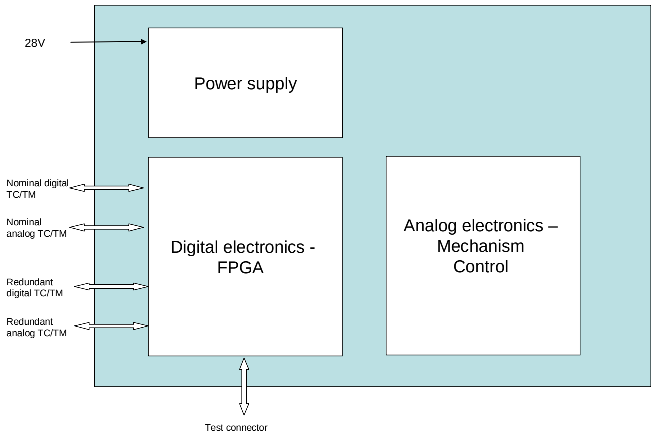

Figure 12: BSME Architecture

4. Evaluation campaigns and electronics allocation

To mitigate the technical risks of this challenging development, two evaluation campaigns were performed first on strain gages mounted on an APA60SM® then on a BreadBoard Model.
An electronic allocation was established.

4.1. Strain gage evaluation campaign

Several tests were performed to qualify the gluing process in regards of:

- The functional performances (with static and dynamic measurement, thermal cycling,),
- Integrity of the piezo ceramic coating (with lifetime, Destructive Part analysis),
- Cleanliness and outgassing (including TML/RML/CVCM characterization).

Strain gages response is measured when a step voltage of 120V is applied on the piezo. Due to piezo creep effect, displacement should then follow the next formulae (Eq.6).

$$\Delta L(t) \approx \Delta L_{t=0.1}\left[1+\gamma \times \log\left(\frac{t}{0.1}\right)\right] \qquad (6)$$

With $\Delta L_{t=0.1}$, the stroke after 0.1seconds; γ, the piezo coefficient and t, the time varying.

Previously, this creep effect could not be monitored using strain gages based on standard gluing process (Fig. 13a). Measurement accuracy is significantly improved with the optimized gluing and now allows observing the creep effect (Fig. 13b).

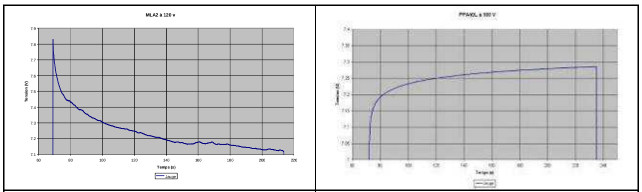

a- Qualitative response with non optimised process	*b- Qualitative response with improved process*

Figure 13: Creep measurement (0-120V step response) using standard and improved gluing process.

Specific tests were conducted to verify that no degradation occurs when gluing the strain gages directly on the piezoceramic. In particular, leakage current has been checked during 2000 Hours under max DC voltage with 40%, 60% and 80% of RH to valid the efficiency of the coating.

The strain gage transducers are known as very accurate for short term period but usually show slow deviation over time. This could affect the WB balancing (i.e. residual offset) during the on orbit time.
In order to validate this ageing behaviour, strain gages resistance was monitored over 1 month for several

specimens (Fig. 14).

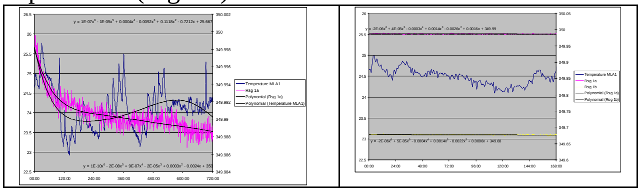

a- *Entire measurement from t0→to+1month.(Resistance curve is Magenta)*	b- *Extract after 1 month on 7 days period.*

Figure 14: Ageing characterisation of SG behavior

This characterisation showed the creep of the glue and the reduction of the variation rate after 1 month. Low rates could be reached on a shorter period by accelerating the phenomena using cycling.

This campaign was successful and the strain gage process was qualified.

4.2. BreadBoard Model results

A BBM has been manufactured. This model is limited to the Tip-Tilt mechanism and a functional IB board (Fig. 15).

Figure 15: Realisation of the Tip-Tilt mechanism BBM

A Ground Support Equipment (GSE), based on standard products from Cedrat Technologies, is used for:

- Piezo driving,
- Strain gages signals conditioning,
- Close loop control (digital controller).

The BBM then was used to verify the BSM capability to achieve the performance requirements for:

- The angular range and the mechanical resonant frequency (Tab. 4) ,
- The linearity of the movement (Tab. 5),
- The repeatability (Fig. 16 and Tab. 5)
- The thermal residual drift (Fig. 17 and Tab. 5).

Angular measurements were conducted using an autocollimator. The system was configured to achieve a differential measurement between the TTM base and the mirror.

Parameters	**Rx**	**Ry**
Full Stroke in open loop (µrad)	4724 @171V	3622 @173V
Full Stroke in closed loop (µrad)	4193 @7.5V	3046 @7.5V
Cross coupling in open loop (µrad)	43.3	46.2
First resonant frequency (Hz)	2121	2390

Table 4: Extract of the range and first resonant frequency measurements

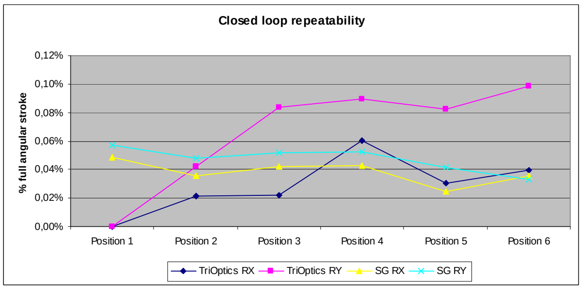

Figure 16: Repeatability results for any identical angle in closed loop

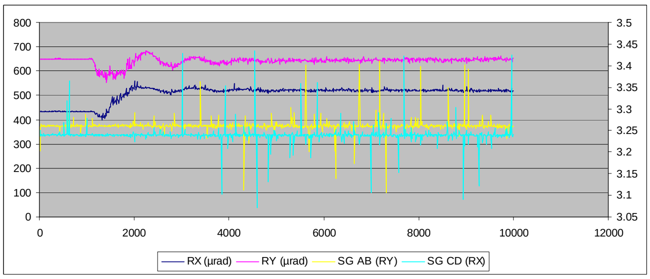

Figure 17: Thermal stability for large excursion in closed loop – 24°C→40°C

Tab. 5 summarizes the measured performances in regards of the mechanical angles.

Parameters	**Unit**		**Req.**	**Value**
Linearity @14°C and @40°C	-	Rx	1 +/-5%	0.999→1.027
		Ry	1 +/-5%	0.988→1.03
Thermal stability	µrad/°K	Rx	5	4.81
		Ry	5	0.19
Repeatability	µrad	Rx	70	4
		Ry	50	1.8

Table 5: Summarises of measured performances on BBM (Mechanical angles)

4.3. Electronic and Optical GSE allocation

In addition to the BBM results, Sodern studied the complementary electronic and Optical GSE contribution to thermal sensitivity. Sodern estimates that the added contribution is equal to 2µRad/K. The global thermal sensitivity is compliant to the global budget.

4.4. BSA consumption

The table hereunder presents the estimated consumption, considering a worst case, compared with the consumption requirement.

Sub-assembly	Calculated power consumption (W)	
	Typ	Requirement
BSM	0.14	< 0.20
BSFE	0.32	< 1.30
BSME	3.10	< 4.50
BSA	3.56	< 6.00

Table 6: Estimated power consumption

The estimated consumption is compliant to the specification.

5. Further development and conclusion

The BSA detailed design and associated justification is now over. The theoretical performances are consistent with the requirements. Functional validations were conducted on breadboard models. The results were on-line with the expected performances and validated the technical choices and manufacturing processes.

The next phases are the EQM manufacturing and complete qualification in regards of the functional and environmental requirements.
Finally, 2 FMs will be delivered for ATLID instruments.

This new mechanism shows the pertinence of APA® with Strain Gage technology for demanding space applications. The concurrent development between Cedrat Technologies and Sodern allowed the design of a challenging multidisciplinary system on a short time schedule.

6. REFERENCES

1 Hélière, A. , Gelsthorpe, R., Le Hors, L., Toulemont, Y., ICSO 2012, ATLID, the atmospheric LIDAR on board the EarthCARE satellite

2 Laurent P., Clairon A., Salomon C., Massonet D., 2010, CNES, PH-DS.0.161.CNS, Pharao synthesis document.

3 Barillot, F., Fabbro, H., .Le Letty, R. , Guay, Ph. (2003) 10th European Space Mechanisms and Tribology Symposium. Design and tests of normally centred piezo mechanisms and their control electronic